Rheology of highly swollen chitosan/polyacrylate hydrogels

H. Jiang[a,b], W. Su[a,c], P.T. Mather[a], T.J. Bunning[a,*]

[a]*Materials and Manufacturing Directorate, AFRL/MLBP and AFRL/MLPJ, Wright Patterson AFB, OH 45433-7702, USA*
[b]*Anteon Inc., Dayton, OH 45431, USA*
[c]*Technical Management Concepts, Inc., Beavercreek, OH, USA*

In honor of Professor Ronald K. Eby's 70th birthday: to a great friend, colleague, and mentor

Abstract

Recently we reported on chitosan hydrogel systems having excellent laser damage resistance. The measured laser damage threshold (LDT) was better than BK7 glass and quartz, commonly used inorganic optical materials, and 20 to 35 times higher than commercial PMMA, a popular polymer optical material. In this study, we continue our investigation of the phase transition behavior of water within the hydrogels by means of oscillatory shear rheology. The crystallization and melting behavior of ice in these hydrogels is greatly affected by the internal structure of the network. Changes in this structure are probed by comparing differences in the rheological measurements at temperatures above and below freezing. Trends among the measured shear storage modulus (G'), shear loss modulus (G'') and shear loss tangent (tan δ) are shown to be related to the mobility of water within the gels. The activation energy associated with the melting of ice in a particular hydrogel was found to be significantly higher than the melting enthalpy of pure ice, suggesting imperfection in the ice crystals and/or a low degree of crystallinity in the hydrogel. © 1999 Elsevier Science Ltd. All rights reserved.

Keywords: Hydrogel; Chitosan; Rheology

1. Introduction

The rapid increase in the use of lasers in high-tech applications such as electro-optical equipment and medical instruments has resulted in a strong interest in materials which can survive high laser radiation power [1–5]. It is also well recognized that the failure of many laser devices is caused by important optical components being destroyed by laser-induced damage [3,6]. Polymer optical materials, such as polymethyl methacrylate (PMMA) and polycarbonates (PC), have substantially lower laser damage resistance than many inorganic compounds [3,7–10]. Many attempts have been made to improve the laser damage resistance of polymer materials in the last two decades [11–13]. Recently, our lab reported that hydrogel systems based on chitosan polymers have emerged as a new class of host materials for laser applications [14,15]. These chitosan hydrogel systems show excellent laser damage thresholds (LDT) of 290–450 µJ, 20 to 35 times higher than that of commercial PMMA (16 µJ). The measured LDT is also substantially better than BK7 glass (68 µJ) and optical grade quartz (272 µJ), widely used inorganic optical materials [15], when tested in identical experimental configurations.

The water in a hydrogel systems has been shown to play a key role in the enhancement of the LDT, with LDT increasing with increasing water content for these gel systems. These gel systems are considered crosslinked macromolecular networks which form a heterogeneous microporous structure holding a large amount of water [15]. This water has been shown to be either bound in part by hydrophilic interactions with the internal polymer surfaces or associated to different degrees depending on the internal structure. The substantially higher mobility of water in the gels compared to solid polymer molecules leads to self-healing and a large energy dissipation capability upon laser irradiation. Water adjacent to the irradiated spot can quickly flow into microvacancies resulting from the vaporization (and/or decomposition) of water at the laser focus area. Thus, the water's micro-Brownian movements efficiently remove the heat energy induced by the laser radiation. This energy transfer is enhanced as the amount of bound water is decreased. Thus, as the polymer network density is decreased, behavior approaching that of pure water is observed.

* Corresponding author. Tel.: + 1-937-255-3808; fax: + 1-937-255-1128.
E-mail address: bunnintj@ml.wpafb.af.mil (T.J. Bunning)

Table 1
A list of the measured samples of the modified chitosan samples. Different chitosan hydrogel samples examined

Water content (%)	Crosslinker ratio (%)		
	0.75	1.25	2.5
50	Sample I	Sample II	Sample III
75	Sample IV	Sample V	Sample VI
86	Sample VII	Sample VIII	Sample IX

In this study, we continue our investigation of the phase transition of water within these gels and the effect of crosslinking. We have used oscillatory shear rheological measurements to probe the local environment due to its high sensitivity to molecular relaxation processes. Specifically, we infer information regarding the ratio of bound to unbound (weakly associated) water by examining changes in the melting behavior and relating these to local differences in the internal structure. Different temperature and frequency sweeps were performed in an attempt to further understand the relationship between the structure and properties. These results are compared to the conclusions made in our recent studies using DSC measurements [15] with regard to the high LDT observed.

2. Experimental procedures

As shown in Table 1, nine chitosan/polyacrylate hydrogels were prepared with variation in both water content and crosslinker ratio. Three different water contents and crosslinker ratios were examined. Details about the chemistry and basic characterization as well as the general procedures for preparation of the chitosan hydrogel system can be obtained in Ref. [15]. The water content was measured gravimetrically by vacuum drying (GVD). Thermal gravimetric analysis (TGA) was used to confirm the water content as measured with GVD. Strong agreement between the TGA and GVD measurements were found as indicated by comparing the water contents of sample I: 50% (GVD) and 44% (TGA); sample V: 75% (GVD) and 73% (TGA); and sample IX: 86% (GVD) and 85% (TGA).

The oscillatory shear rheological measurements were performed on a dynamic mechanical spectrometer (Rheometrics Model RDA-II). An oscillatory strain is applied to the samples (Eq. (1)),

$$\gamma(t) = \gamma_0 \cos(\omega t) \tag{1}$$

and the shear stress (Eq. (2)) is measured from the resultant torque.

$$\sigma(t) = G^* \gamma_0 \cos(\omega t + \delta). \tag{2}$$

Eqs. (3) and (4) are then used to calculate the characteristic storage and loss moduli from the complex modulus, G^*, and phase angle δ:

$$G' = G^* \cos \delta, \tag{3}$$

and

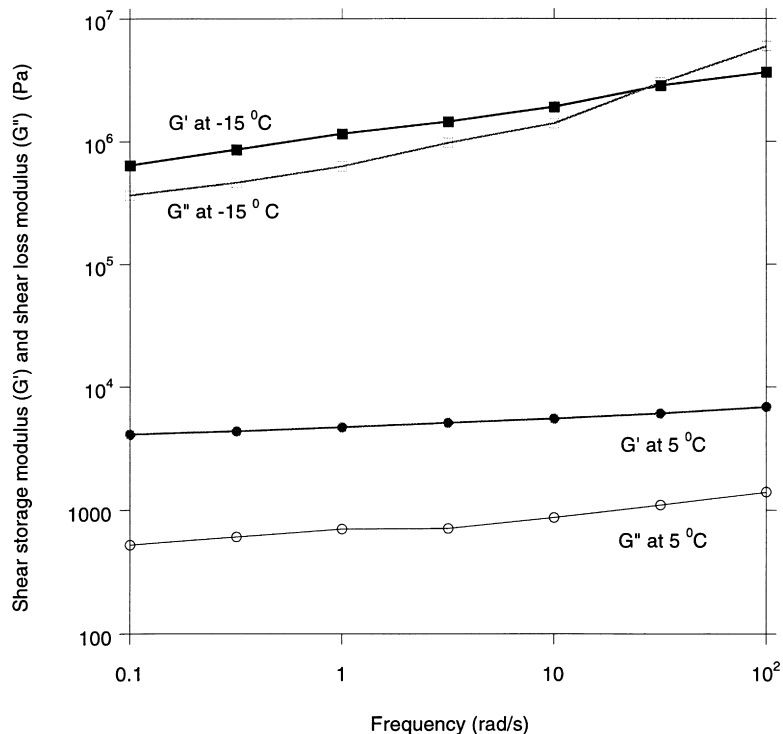$$G'' = G^* \sin \delta. \tag{4}$$

Fig. 1. Representative logarithm plot of G' and G' vs. frequency of sample VII at − 15 and 5°C.
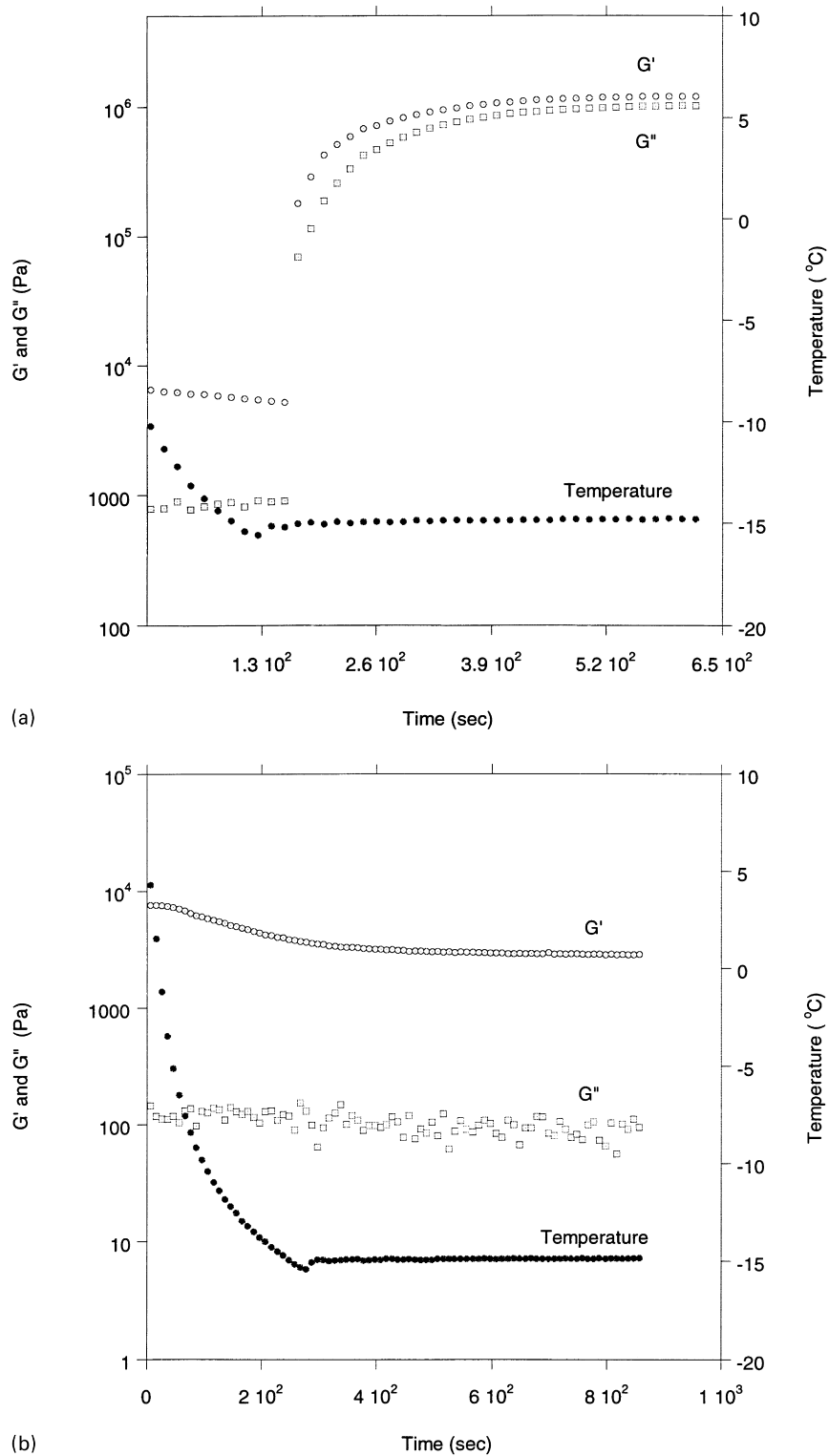
(a)

(b)

Fig. 2. Time evolution of shear storage modulus (open circles), loss modulus (open squares), along with temperature (closed squares) during cooling and subsequent annealing at $T = -15°C$ for (a) sample IX and (b) sample I.

For all the hydrogel samples, a 2.5 cm diameter disc was used except for the air-dried sample (water content of 7%), where a 5 mm disc was used as a result of volume shrinkage. The thickness of all samples was approximately 1 mm. The applied strain was 1%. The shear frequency varied from 0.1 to 100 rad/s and temperature sweeps spanned from -20 to $+20°C$ with different heating rates from 0.5 to 2°C/min. A home-made acetone dry-ice heat exchanger was used to
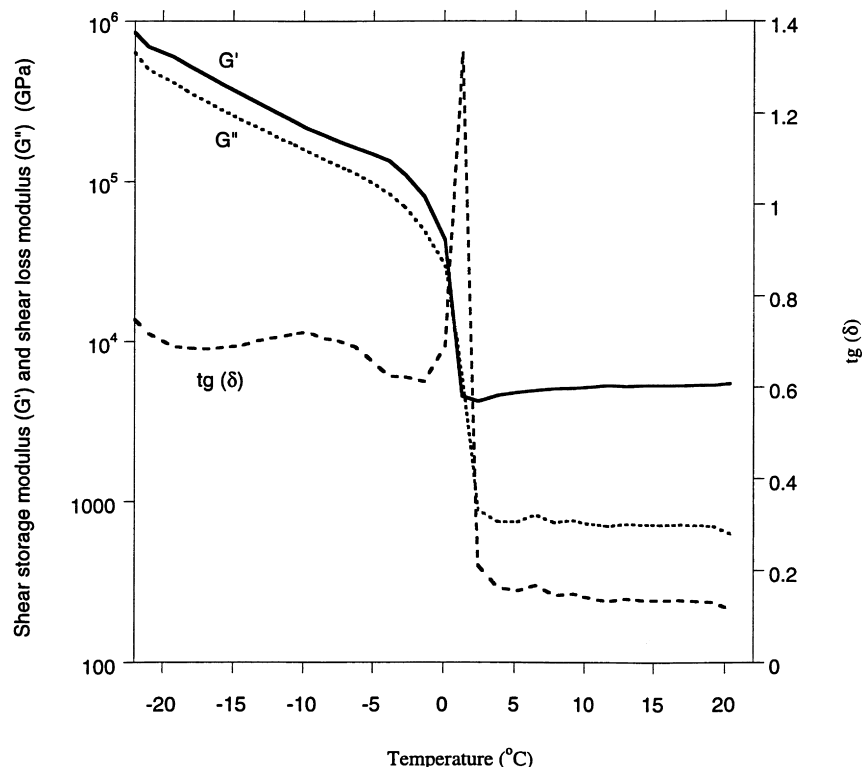
Fig. 3. Temperature dependence of shear storage modulus (solid line), loss modulus (fine dash), and loss tangent (coarse dashed line) during heating of hydrogel sample VIII at 4°C/min and using an oscillation frequency of 0.1 rad/s.

provide cooling for the N_2 flow in the sample environmental chamber. A uniform thin layer of silicone vacuum grease was applied to the outer-circular edges of the shear-discs to prevent water loss from the samples. This grease was proven to have a negligible effect on the measured rheological properties. Inspection of post-rheology samples confirmed the prevention of water loss.

3. Results and discussion

Fig. 1 shows a representative frequency spectrum for sample VII at $T = 5$ and $- 15°C$. At $T = 5°C$, the material is gel-like, with storage and loss moduli versus frequency curves being approximately parallel. Cooling this sample to $- 20°C$ and then heating to $- 15°C$ dramatically affects the rheological spectrum (Fig. 1). A large increase in the moduli magnitude occurs, along with the appearance of a crossing of G' and G'' at $\omega \approx 25$ rad/s. The large increase in moduli at the lower temperature is attributed to the formation of ice.

Cooling the hydrogel samples to $- 15°C$ results in a time evolution of storage and loss modulus that depends strongly on the weight fraction of water present in the hydrogels. Shown in Fig. 2(a) is the time dependence of the shear storage and loss modulus for sample IX (high water content) during cooling from room temperature to $- 15°C$ at a rate of approximately 10°C/min and subsequent annealing at this temperature. It can be seen from Fig. 2(a) that following a

period of weak temperature dependence, the storage and loss moduli are observed to increase by two and three orders of magnitude, respectively, over the course of approximately 5 min. This increase is attributed to crystallization of water within the hydrogel. Sample I (low water content) shows contrasting behavior, as shown in Fig. 2(b). In this case, even after annealing at $T = - 15°C$ for 10 min, no rheological evidence for crystallization is observed, indicating that a minimum water content in the hydrogels, $w >$ 50% (approximately), is required for crystallization to occur at $- 15°C$. Based on these results, the temperature sweep experiments that are discussed later were initiated only after an isothermal steady state was achieved, thereby ensuring completion of any water crystallization.

Fig. 3 gives a typical result of the temperature-dependent rheological properties for the hydrogels, in this case sample VIII. For this experiment, the oscillation frequency was 0.1 rad/s and the temperature was cooled to $- 20°C$, annealed for 5 min, then heated from $- 20$ to $20°C$ at a rate of 0.5°C/min. Fig. 3 indicates that below $T \cong 0°C$ (approximate melting point of ice, T_{mw}), the hydrogel is a viscoelastic solid with both the shear storage modulus (G') and shear loss modulus (G'') being strongly temperature dependent and comparable in magnitude ~ 0.1–1.0 MPa. The loss tangent is also substantial, maintaining a value of approximately 0.7 or more. A small maximum in the loss tangent, potentially derived from "melting" of imperfect or bound ice crystals, is also indicated at $- 5°C$ [16].
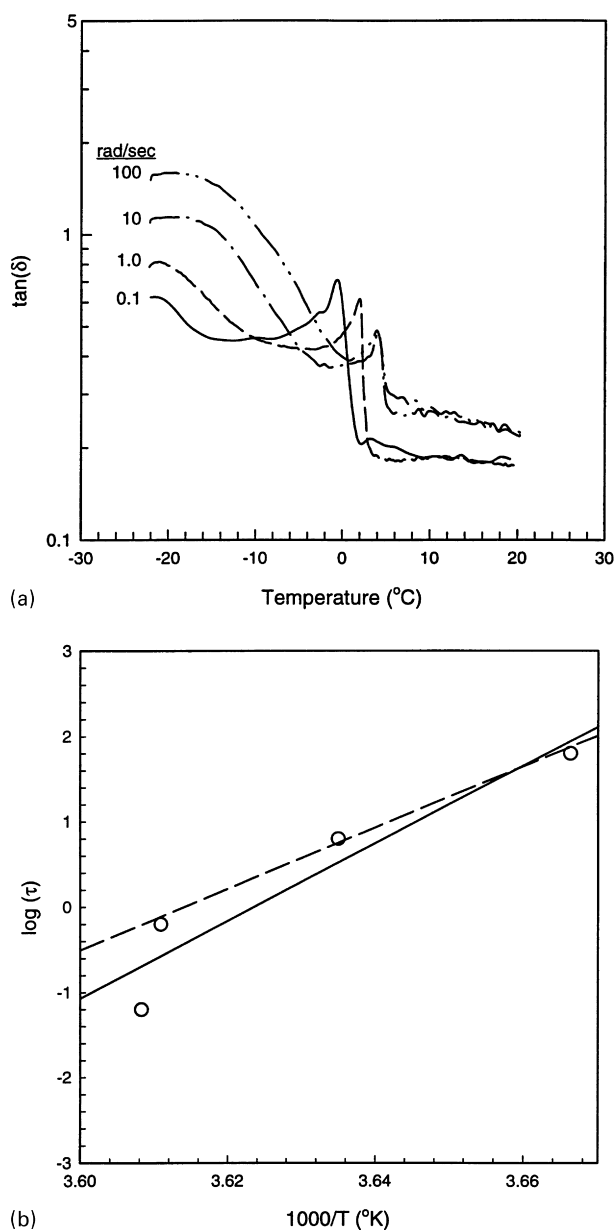
(a)

(b)

Fig. 4. (a) Loss tangent versus temperature at various frequencies, $\omega = 0.1$, 1.0, 10 and 100 rad/s, using sample II; (b) Arrhenius plot for measurement of relaxation activation energy.

Increasing the temperature above $T \approx 1.4°C$, a strong mechanical relaxation indicated by the large peak in the shear loss tangent (tan $\delta = G''/G'$, $\frown$ 1.35) is observed. A significant drop in the shear moduli to values typical of a soft, swollen polymer network (500–1000 Pa) occurs. A surprising observation is that the magnitude of the loss tangent for $T > T_{mw}$ is *lower* than that for $T < T_{mw}$ by a factor of about 6. This indicates that the dissipation of energy, over a wide range of frequencies is higher for the hydrogel which contains some level of frozen water than for the gel containing liquid water. The large loss tangent (with an upward curvature) at $T < T_{mw}$, suggests the existence of a secondary (β) mechanical relaxation, such as that observed

in swollen polystyrene [17] and in semicrystalline polymers [18]. However, the loss tangent peak for such a relaxation must occur at a temperature lower than our experimental limitation of $T = -22°C$. Because measurements on dried hydrogel samples (not shown) display no evidence for mechanical relaxation over the range $-22 < T < 20°C$, we are led to conclude that the secondary relaxation is related to motion and energy dissipation within the crystallized water regions, analogous to the α-relaxation in low-density polyethylene attributed to molecular reorientations within the crystals [19].

A larger shear modulus for temperatures below T_{mw}, as seen in Fig. 3, is expected as the magnitude of the shear modulus for ice is approximately 4 GPa [16], a value comparable to solid polymers [20]. Such a modulus is five orders of magnitude larger than the observed shear storage modulus above T_{mw} and four orders of magnitude larger than the observed value below T_{mw}. This disparity in moduli suggests that the degree of crystallinity and/or the perfection of these ice crystals in sample VIII (and all of our hydrogel samples) is actually quite low.

To study the melting behavior in more detail, we examined the dependence of shear loss tangent on temperature (through the melting point) for a wide range of oscillation frequencies. The results typical of all the hydrogels were exhibited by sample II, shown in Fig. 4(a). We observe a rightward temperature shift with increasing frequency for both the primary relaxations near $T = 0°C$, but also a large shoulder of the secondary relaxation discussed before in reference to Fig. 3. As is expected for the mechanical relaxation of viscoelastic materials, increasing the oscillation frequency results in an increase in the temperature of the relaxation; i.e. a shifting of the loss tangent peak to higher temperatures. The magnitude of such a shift is directly related to the activation energy of the relaxation within the framework of an Arrhenius thermal model. To determine the activation energy, ΔH, a plot of $\log(1/\omega)$ vs. $1000/T$ was constructed, based on the Arrhenius model:

$$\tau = \tau_0 \exp\left(\frac{\Delta H}{RT}\right) \qquad (5)$$

and therefore

$$\log(\tau) = \log(\tau_0) + \frac{\Delta H}{RT}, \qquad (6)$$

where we have used $1/\omega = \tau$. This plot is shown in Fig. 4(b) and results in a value of $\Delta H \cong 90 \pm 10$ kcal/mol (71 kcal/mol if the skewed high frequency data point is discarded); the large estimation error being derived by the deviation of the highest frequency point from the straight line. We note that this activation energy is nearly two orders of magnitude larger than the melting enthalpy of ice (1.4 kcal/mol), although equivalence is not expected.

We have also examined the temperature dependence of the shear storage modulus for the hydrogels and now discuss the results for samples III, VI, and IX with varying water
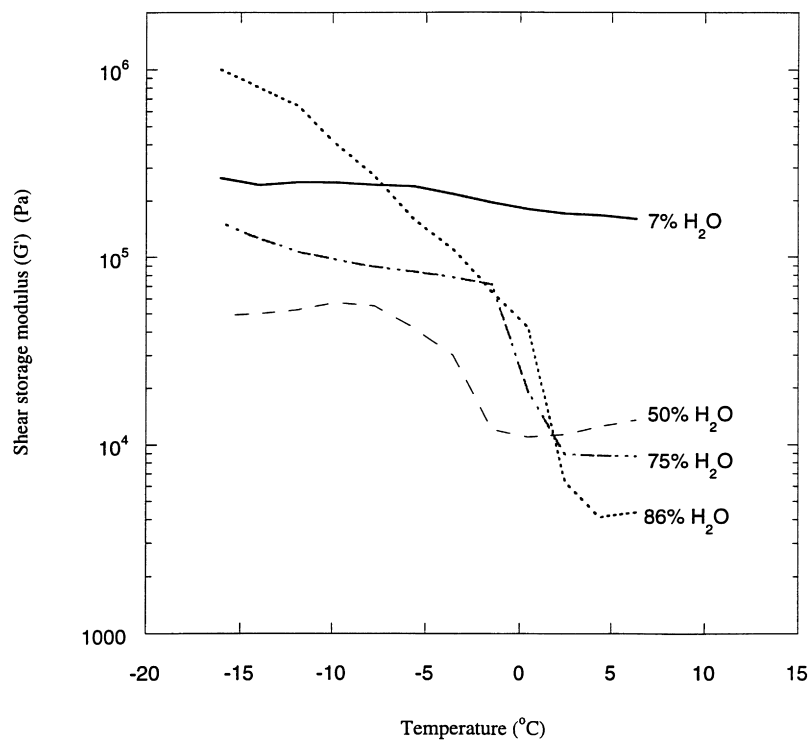
Fig. 5. Changes in shear storage modulus (G') with different water contents for hydrogel samples III, VI, IX and air-dried IX. The rheological measurement was performed at the frequency of 1 rad/s.
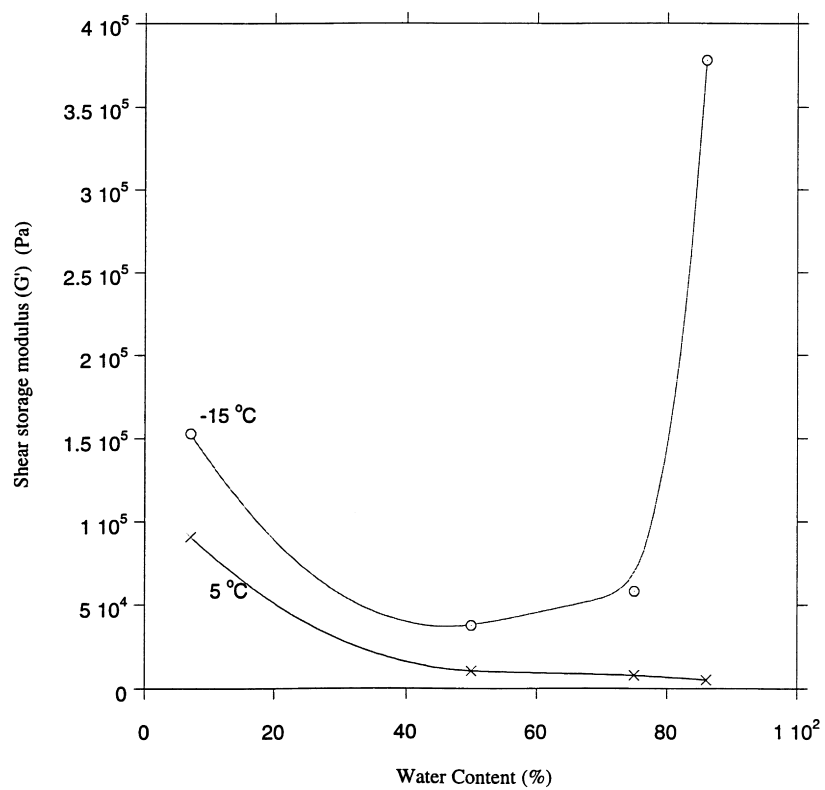

Fig. 6. Shear storage modulus (G') changes with water content at 5 and $-15°C$ for samples I, IV, and VII, and air-dried sample VII. The rheological measurement was performed at frequency of 0.1 rad/s.
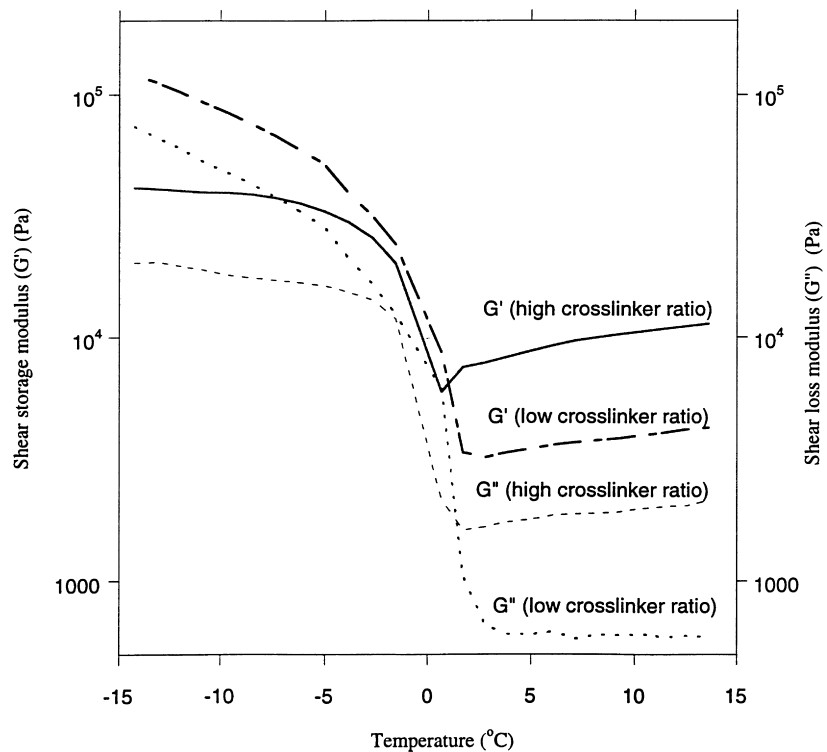
Fig. 7. A comparison of G' and $G($ between low (0.75%) and high crosslinker ratios (2.5%) for hydrogel samples IV and VI at frequency of 0.1 rad/s.
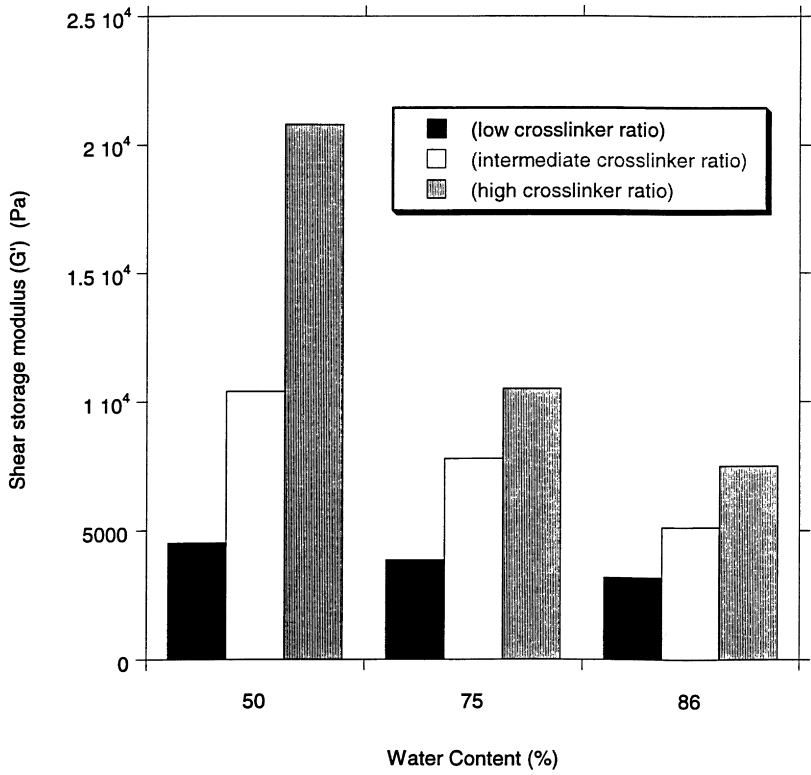
Fig. 8. The rheological results of the modified chitosan gels describing the effects of water content and crosslinking density on G' at 10°C.
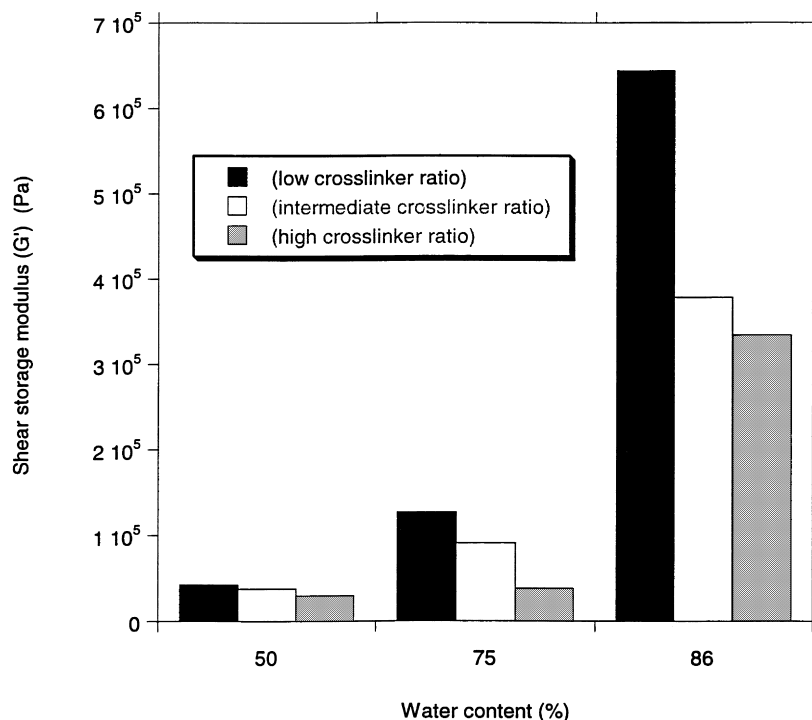
Fig. 9. The rheological results of the modified chitosan gels describing the effects of water content and crosslinking density on G'' at $-15°C$.

contents of 50, 75 and 86%, respectively, and an air-dried sample IX (with a water content of 7%). All of these samples had the same crosslinker ratio (2.5%). Fig. 5 is a plot of storage modulus versus temperature for these four samples, where an oscillation frequency of 1 rad/s was employed. There is a mechanical relaxation (step-down in storage modulus) near $T = 0°C$ for the three hydrated samples. Above T_{mw}, increasing the water content from 7 to 50% results in a significant *decrease* in the storage modulus, G', as expected because of the swelling effect of water on the hydrogels as shown in Fig. 6. Upon increasing the water content further from 50 to 86%, the value of G' decreases gradually as the material becomes softer.

A more complicated behavior is observed at temperatures below T_{mw}. As summarized in Fig. 6, G' first decreases and then increases with increasing water content, with a significant drop occurring between 7 and 50% samples. This non-monotonic behavior results from the saturation of association sites on the hydrophilic polymer with water (bound water). Below a water content of 50%, added water binds to the polymer, apparently plasticizing the material, while above 50%, an increase in the water content does not add to the amount of bound water but rather adds to the amount of unbound (weakly associated) water. Below T_{mw}, this unbound/weakly-associated water is capable of crystallizing locally and thus the modulus increases commensurately. Such behavior is strongly consistent with our previous work [15] wherein DSC measurements showed no melting endotherm or crystallization exotherm for samples with less than 50% water. This behavior is manifested here as an

increase in the modulus values as the volume fraction of ice increases.

The influence of crosslinker ratio on storage and loss modulus was also studied. Fig. 7 shows the change of the storage and loss shear moduli; G' and G'', respectively, with temperature for samples IV and VI. Both samples have intermediate water content (75%) but different crosslinker ratios (0.75 and 2.5%, respectively). For temperatures above T_{mw}, the magnitudes of both G' and G'' for sample VI (with high crosslinker ratio) are larger than G' and G'' of sample IV (with low crosslinker ratio). Clearly, the increase in crosslinking densifies the network and thus its mechanical stiffness increases. The increase in crosslinker ratio leads to an increase in the gel's storage modulus through the relationship [21,22]

$$G'_R = \frac{\rho RT}{M_c} \tag{7}$$

where G'_R is the relaxed rubbery modulus, r is the density, R is the universal gas constant, T is the temperature, and M_c is the molecular weight between crosslinks. An alternative form of Eq. (7) is

$$G'_R = \nu RT, \tag{8}$$

where ν is the number of crosslink sites per unit volume. These simple relationships do not account for contributions from trapped entanglements which may be introduced during the crosslinking reaction. Nevertheless, we have used Eq. (8) with the data shown in Fig. 7 at $T = 10°C$ to estimate the ratio of crosslink densities, $R = \nu_{HCD}/\nu_{LCD}$

where HCD and LCD correspond to high and low crosslink densities, respectively. This ratio can be compared to the ratio obtained from the gel synthesis, $R^s = w_{HCD}/w_{LCD}$, where w is the weight percentage of crosslinking monomer used in the synthesis. The values of $R = 2.73$ were found from the rheology data and $R^s = 3.33$ from the theoretical calculation. The slight difference in these ratios is likely due to the use of weight percentage in the equation for R^s and from the lack of control over complete incorporation of crosslinking monomers in the gel synthesis. However, the observation that $R \approx R^s$ allows us to conclude that the rubbery modulus of the hydrogels ($T > T_{mw}$) is easily controlled by the crosslinker ratio, as anticipated.

For temperatures below T_{mw}, the storage and loss moduli of sample IV are higher than those from sample VI as shown in Fig. 7. This suggests that crystallization of water in samples of lower crosslink concentration occurs to a greater extent as compared with samples of higher crosslink concentration. As the crosslink density is increased, the ability of ice to crystallize is hindered. The ratio of bound to unbound water increases and the resulting decrease in the amount of ice crystallization leads to lower modulus values. This observation is again fully consistent with our recent DSC findings [15] wherein separate exothermic peaks were observed on cooling, each successive peak being attributed to crystallization of water with increasing association strength. The relative amounts of each type depended on the relative crosslink density and the amount of water.

We summarize the experimental results for samples I–IX in Figs. 8 and 9 for temperatures above and below T_{mw}, respectively. In Fig. 8, for $T = 10°C$, increasing in the water content causes the storage modulus, G', to become consistently smaller in magnitude. This is expected as more and more water swells the gels leading to a decrease in the ratio of bound to unbound water. For a given water content, increasing the crosslink concentration increases G', though to a lesser degree, with the largest enhancement being seen for the lower water content samples. At $T = -15°C$, the opposite trends are observed, as shown in Fig. 9. This is again attributed to the presence of more unbound water (relative to bound water) for water contents $> 50\%$. This water can crystallize and as more and more is added, the number, size, and perfection of the ice crystals increases which leads to an increase in storage modulus. At a given water content, increase in the crosslinker ratio decreases G', apparently a result of suppression in the amount of ice that can be formed.

This rheological data supports the concepts of water–polymer interactions as previously discussed. Hydrogels consist of a hydrophilic macromolecular network which is swollen by water. Inside the hydrogels the states of water are complicated. The water may exist in a continuum of states between two extreme cases: (1) strongly associated water which can never form ice crystals, and (2) phase-separated water nearly unaffected by the polymer environment [23]. When the water is removed, the network collapses and the macromolecular chains may organize to form amorphous and/or crystalline domains. In this case, most of the remaining resident water would be bound by the hydrophilic moieties on the polymer chains. As more and more water is added, the ratio of completely bound water to unbound (yet somewhat associated) water decreases. Above a water content of approximately 50%, enough unbound water is present to crystallize locally upon cooling. The rheology measurements support this picture both above and below the crystallization temperatures of ice. Below 0°C, both the storage and loss moduli increase as the amount of water is increased above 50% as a result of the increased amount of ice. Below 50% a small change occurs as all water is effectively bound by the polymer network thereby hindering ice formation. Above room temperature, these larger regions of unbound water in samples with $> 50\%$ water lead to the lowest storage and loss moduli values. For a given water content, as crosslink density is increased the ratio of bound to unbound water increases. These differences are also manifested in the values of the storage and loss moduli. Increase in the crosslink density above the room temperature provides more rigidity to the structure and thus the moduli values increase. Below 0°C, a higher crosslink density suppresses the formation of ice and thus lower modulus values are observed as density is increased. Thus the rheology measurements yield information of the nature of the water–polymer interaction. By examining rheological changes resulting from the phase transition of water/ice, differences in the internal structure can be probed.

4. Conclusion

An oscillatory shear rheological study with variation in temperature and frequency was performed to further understand the phase behavior and crosslinking of the modified chitosan gels which exhibit excellent LDT. It was observed that all the measured viscoelastic properties, including G', G'' and tan δ, are significantly influenced by the water phase transition which occurs with decrease in temperature. If the water content exceeds a critical level in the hydrogels, both G' and G'' of the modified chitosan hydrogels have a sharp increase at $T < T_{mw}$, because of ice formation, and the loss tangent (tan δ) shows a strong relaxation peak around T_{mw}. In addition, for $T < T_{mw}$ both G' and G' increase with increasing water content in the hydrogel; however, both decrease when $T > T_{mw}$. Increasing the crosslinker ratio causes the mechanical stiffness of the network (G') to increase when the $T > T_{mw}$, but decrease when $T < T_{mw}$, as a result of inhibition of water phase transition. Based on these results, we suggest that the changes of the viscoelastic properties bear a close relationship with the water states and mobility in the hydrogels which in turn play a significant role in determining the LDT of the gel materials.

References

[1] Soffer BH, McFarland BB. Appl Phys Lett 1967;10:266.

[2] Ermakov BA. Opto-electronic devices with lasers. Leningrad: Nauka, 1982.

[3] Manenkov AA, Maslyukov AP, Matyushin GA, Nechitailo VS. SPIE 1994;2115:136.

[4] Sastre R, Costela A. Adv Mater 1995;7(2):198.

[5] Duarte FJ. Laser Focus World, Vol. 187, May 1995.

[6] Manenkov AA, Matyushin GA, Nechitailo VS, Prokhorov AM, Tsaprilov AS. Optical Engng 1983;22(4):400.

[7] O'Connell RM, Saito TT. Optical Engng 1983;22(4):393.

[8] Dyumaev KM, Manenkov AA, Maslyukov AP, Matyushin GA, Nechitailo VS, Prokhorov AM. Sov J Quant Electron 1983;13(4):503.

[9] Glass AJ, Guenther AH. Appl Optics 1977;16(5):1214.

[10] Balachandran RM, Pacheco DP, Lawandy NM. Appl Optics 1996;35(4):640.

[11] Bondar MV, Przhonskaya OV, Tikhonov EA. Sov Phys Tech Phys 1988;33(3):309.

[12] Butenin AV, Kogan BY. Sov J Quant Electron 1986;16(10):1422.

[13] De Rosa ME, Su W, Krein D, Brant MC, McLean DG. SPIE 1997;3146:134.

[14] Jiang H, Su W, Brant M, Tomlin D, Bunning T. MRS Symposium Proceedings 1997;479:129.

[15] Jiang H, Su W, Brant M, DeRosa M. Bunning. T. J Polym Sci Polym Phys Ed 1999, in press.

[16] Davidson D. Gas hydrates as clathrate ices. In: Cox J, editor. Natural gas hydrates-properties, occurrence and recovery, Woburn, MA: Butterworth, 1983. p. 1.

[17] Illers KH, Jenckel E. Rheol Acta 1958;1:322.

[18] McCrum NG, Read BE, Williams G. Anelastic and dielectric effects in polymeric solids. London: Wiley, 1967.

[19] Rempel RC, et al. J Appl Phys 1957;28:1082.

[20] Ward IM. Mechanical properties of solid polymers. New York: Wiley-Interscience, 1971.

[21] Sperling LH. Introduction to physical polymer science. New York: Wiley, 1986.

[22] Ilavsky M. Advances in Polymer Science 1993;109:173.

[23] Pathmanathan K, Johure GP. J Polym Sci Pt B Polym Phys 1990;28:675.